

The nature of Feshbach molecules in Bose-Einstein condensates

T. Köhler,¹ T. Gasenzer,² P. S. Julienne,³ and K. Burnett¹

¹*Clarendon Laboratory, Department of Physics, University of Oxford, Oxford, OX1 3PU, United Kingdom*

²*Institut für Theoretische Physik, Philosophenweg 16, 69120 Heidelberg, Germany*

³*Atomic Physics Division, National Institute of Standards and Technology,
100 Bureau Drive Stop 8423, Gaithersburg, Maryland 20899-8423*

(Dated: December 7, 2018)

We discuss the long range nature of the molecules produced in recent experiments on molecular Bose-Einstein condensation. The properties of these molecules depend on the full two-body Hamiltonian and not just on the states of the system in the absence of interchannel couplings. The very long range nature of the state is crucial to the efficiency of production in the experiments. Our many-body treatment of the gas accounts for the full binary physics and describes properly how these molecular condensates can be directly probed.

PACS numbers: 03.75.Kk, 34.50.-s, 36.90.+f, 05.30.-d

Bose-Einstein condensation of molecules is an exciting challenge and opportunity in the physics of ultracold gases. As direct laser cooling of molecules is largely prevented by their densely lying rovibrational energy levels, several approaches now focus on the association of atoms in Bose-Einstein condensates. Present techniques are based on photoassociation [1] or magnetic field tunable interactions [2, 3]. The detection of molecular condensates, however, remains a demanding problem. Recent experiments at JILA [4] found evidence for molecular condensation by probing coherence properties of the assembly of atoms plus molecules. The ^{85}Rb condensate was exposed to a sequence of two fast magnetic field pulses in the vicinity of a Feshbach resonance. The pulses were separated by a variable period of time with a stationary magnetic field, termed the evolution period. The observed final densities of gas atoms, i.e. the remnant condensate and a “burst” of comparatively hot atoms, indicated a coherent coupling between atoms and diatomic molecules in a highly excited vibrational state during the evolution period. Several subsequent theoretical studies [5, 6, 7] have concluded that the gas contained a molecular condensate at the end of the pulse sequence. The magnitude of the molecular fraction, and the precise mechanism of producing the molecules are a matter of continuing controversy [8, 9]. To settle this issue the next generation of experiments could determine the coherent superposition of atomic and molecular components by directly detecting the molecules. The efficiency of different detection schemes based on laser excitation [10] depends sensitively on the number of molecules and the wave functions of the diatomic bound states produced by a magnetic field pulse.

In this letter we shall give a full description of these wave functions for typical experimental magnetic field strengths and determine the molecular component in the evolution period of the pulse sequence. In particular, we shall show explicitly that the wave functions of the molecules have a spatial extent of the order of the scat-

tering length. At the magnetic field strengths closest to resonance this length scale even becomes comparable with the mean distance between the atoms in the dilute condensate. Under these conditions a separation of the gas into atoms and diatomic molecules is physically meaningless. The strong binary correlations provided by the long range intermediate molecular states, however, are still crucial for the efficiency of the association of atoms to molecules. In the evolution period the typical static experimental field strengths are sufficiently far from the resonant field that the highly excited diatomic molecules can exist as a metastable entity of the gas. The microscopic many-body approach we apply to determine the molecular fraction [7, 11] accounts for the long range nature of the intermediate molecular states. This approach treats bound and free molecular states formed during the pulse sequence in a unified manner and provides a straightforward understanding of the association of condensate atoms to molecules.

The experimental technique of magnetic field tunable interactions takes advantage of the Zeeman effect in the electronic energy levels of the atoms. In the JILA experiments [4] the ^{85}Rb condensate atoms were prepared in the ($F = 2, m_F = -2$) hyperfine state. Throughout this letter the open s -wave binary scattering channel of two asymptotically free atoms in the ($F = 2, m_F = -2$) state will be denoted as the $\{-2, -2\}$ open channel with an associated reference potential $V_{\text{bg}}(r)$. When the m_F degeneracy of the hyperfine levels is removed by an external magnetic field B the potentials associated with the different asymptotic scattering channels are shifted with respect to each other. Although the $\{-2, -2\}$ open channel is only very weakly coupled to other open channels, it can be strongly coupled to closed channels. A zero-energy scattering resonance occurs when the field-dependent energy $E_{\text{res}}(B)$ of a closed channel vibrational state (a Feshbach resonance level) ϕ_{res} is tuned close to the dissociation threshold energy of $V_{\text{bg}}(r)$. We note that the closed channel state ϕ_{res} is not a stationary state of

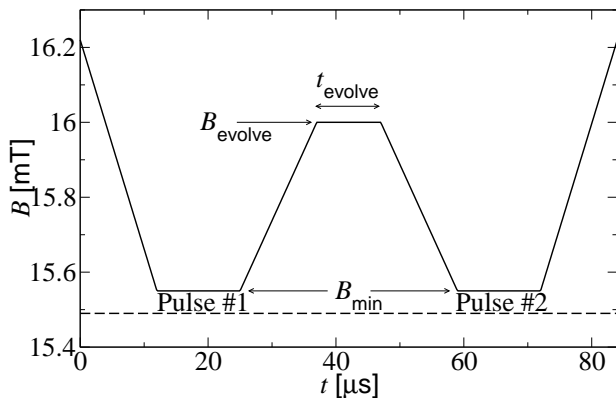


FIG. 1: Scheme of a typical magnetic field pulse shape in the low density ($n_0 = 3.9 \times 10^{12} \text{ cm}^{-3}$) experiments in Ref. [4]. The minimum magnetic field strength of the first and second pulse is $B_{\min} = 15.55 \text{ mT}$. In the evolution period the field strength is chosen as $B_{\text{evolve}} = 16.0 \text{ mT}$. In the course of the experiments the evolution time t_{evolve} as well as B_{evolve} were varied. The dashed line indicates the position of the resonance at $B_0 = 15.49 \text{ mT}$.

the full two-body Hamiltonian, which has a coupling between the channels. If $E_{\text{res}}(B)$ approaches the threshold from below, however, the overall potential matrix supports a shallow multi-channel bound state ϕ_b with energy E_b . This proper stationary molecular state ceases to exist at the position of the resonance ($B_0 = 15.49 \text{ mT}$ [4]), for which the s wave scattering length a of two asymptotically free atoms in the $\{-2, -2\}$ open channel has a singularity. When E_b is sufficiently close to threshold, the component of ϕ_b in the $\{-2, -2\}$ open channel then exhibits the universal form [12] $\exp(-r/a)/r$ at large relative distances of the two atomic constituents of the molecular state.

We shall now describe more fully the long range nature of the molecular states for typical experimental magnetic field strengths in the fast sequence of pulses shown in Fig. 1. To this end we have reduced the complete multi-channel Hamiltonian of the relative motion of two atoms to a two-channel model:

$$H_{2B} = \begin{pmatrix} -\frac{\hbar^2}{m}\nabla^2 + V_{\text{bg}}(r) & W(r) \\ W(r) & -\frac{\hbar^2}{m}\nabla^2 + V_{\text{cl}}(B, r) \end{pmatrix}. \quad (1)$$

Here m is the atomic mass of ^{85}Rb . For the potential in the $\{-2, -2\}$ open channel we use a Lennard-Jones form $V_{\text{bg}}(r) = 4\epsilon [(\sigma/r)^{12} - (\sigma/r)^6]$ with $\sigma = 37.3292 a_{\text{Bohr}}$ ($a_{\text{Bohr}} = 0.052918 \text{ nm}$) and $4\epsilon\sigma^6 = C_6 = 4660 \text{ a.u.}$ [13] ($1 \text{ a.u.} = 0.095734 \text{ yJ nm}^6$). $V_{\text{bg}}(r)$ then reproduces the background scattering length of $a_{\text{bg}} = -450 a_{\text{Bohr}}$ [4]. In accordance with Ref. [14] we model the closed channel potential as $V_{\text{cl}}(B, r) = V_{\text{bg}}(r) + E_{\text{cl}}(B)$, where $E_{\text{cl}}(B)$ follows the dependence of the energy difference of the corresponding Zeeman hyperfine levels on the magnetic

field. We use $\hbar^{-1}\partial E_{\text{cl}}/\partial B = -34.6 \text{ MHz/mT}$. In this simplified model $V_{\text{cl}}(B, r)$ supports only two vibrational states. We assume the excited one to be the resonance state ϕ_{res} which thus satisfies $[-\hbar^2\nabla^2/m + V_{\text{cl}}]\phi_{\text{res}} = E_{\text{res}}\phi_{\text{res}}$. We have chosen the off diagonal potential as [14] $W(r) = \beta \exp(-r/\alpha)$ with $\beta/k_{\text{B}} = 38.5 \text{ mK}$ and $\alpha = 5 a_{\text{Bohr}}$, which gives a width of the resonance of $\Delta B = 1.1 \text{ mT}$ [4]. With this choice of parameters the model also produces the correct shift between the resonance position B_0 and the magnetic field strength B_{res} , where the resonance state crosses the dissociation threshold of $V_{\text{bg}}(r)$ ($E_{\text{res}}(B_{\text{res}}) = 0$). For the ^{85}Rb resonance at $B_0 = 15.49 \text{ mT}$ this shift is negative and of the order of $B_0 - B_{\text{res}} = -0.9 \text{ mT}$, so that the multi-channel bound state ϕ_b persists when the resonance state has crossed the threshold. The corresponding wave functions and negative binding energies are obtained from Eq. (1) by $H_{2B}\phi_b = E_b\phi_b$ and the scattering length is approximated by

$$a(B) = a_{\text{bg}} \left(1 - \frac{\Delta B}{B - B_0} \right). \quad (2)$$

Figure 2 shows the bound state ϕ_b at the magnetic field strengths of $B_{\text{evolve}} = 16.0 \text{ mT}$ and $B_{\min} = 15.55 \text{ mT}$. While B_{evolve} corresponds to the magnetic field during the evolution period of the pulse sequence in Fig. 1, B_{\min} is the magnetic field strength closest to resonance. Both molecular states in Fig. 2 are dominated by their $\{-2, -2\}$ open channel component which contributes 95.3% (99.9%) of the total probability density at B_{evolve} (B_{\min}). For both magnetic field strengths the small closed channel component of ϕ_b assumes the form of the resonance state $\phi_{\text{res}}(r)$. Close to the resonance the bond length of ϕ_b (mean internuclear distance) is on the order of $\langle r \rangle = a/2$. One obtains $\langle r \rangle = 326 a_{\text{Bohr}}$ ($a = 521 a_{\text{Bohr}}$ from Eq. (2)) at B_{evolve} and $\langle r \rangle = 4255 a_{\text{Bohr}}$ ($a = 7800 a_{\text{Bohr}}$ from Eq. (2)) at B_{\min} . At the lowest magnetic field strengths in the pulse sequence in Fig. 1 the spatial extent of the molecules thus becomes comparable with the mean distance between the condensate atoms in the JILA experiments [4], which is of the order of $n_0^{-1/3} = 0.64 \mu\text{m} = 12000 a_{\text{Bohr}}$. Under these conditions, the dilute gas parameter $\sqrt{n_0 a^3}$ is comparable to 1, and one can no longer identify a particular pair of atoms in the gas as a molecule in the state ϕ_b because its molecular wave function would overlap with other gas atoms. One and the same atom could thus contribute to several diatomic molecules. After the pulse sequence and during the evolution period, however, the gas is weakly interacting ($n_0 a^3 \ll 1$) and diatomic molecular bound states are sufficiently confined in space for the number of molecules to be a meaningful quantity.

We shall illustrate the resulting remarkable evolution of the molecular fraction in the JILA experiments [4] with the quantum mechanical many-body description developed in Ref. [7] for a homogeneous gas with the exper-

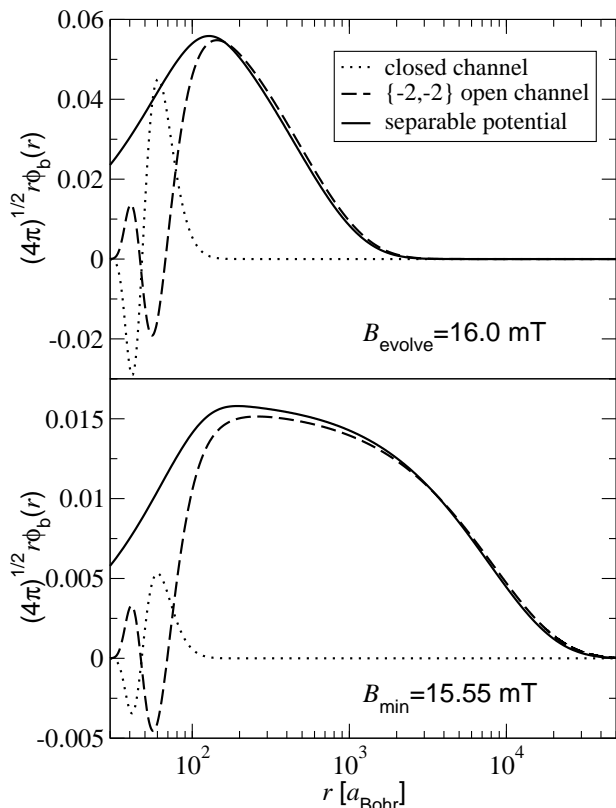


FIG. 2: Coupled-channel bound states at the magnetic field strengths of $B_{\text{evolve}} = 16.0$ mT and $B_{\text{min}} = 15.55$ mT. The radial coordinate is given on a logarithmic scale. The dotted (dashed) curves indicate the closed ($\{-2, -2\}$ open) channel components. The solid curves are the corresponding bound state wave functions of the separable potential in Ref. [7]. The separable potential wave functions agree with the $\{-2, -2\}$ open channel components of the coupled channels bound states at distances large compared to the van der Waals length of $\frac{1}{2}(mC_6/\hbar^2)^{1/4} = 82 a_{\text{Bohr}}$.

imental mean density of $n_0 = 3.9 \times 10^{12} \text{ cm}^{-3}$. The underlying cumulant approach [11, 15] is based on the microscopic many-body Hamiltonian [7] and systematically decouples the exact hierarchy of dynamic equations for quantum correlation functions at any desired degree of accuracy. According to Ref. [7] the dynamics of the condensate mean field Ψ , the molecular fraction of the gas, and the burst of correlated pairs of comparatively hot atoms [4, 7] are all determined by a single nonlinear Schrödinger equation. In the homogeneous gas limit this has the form:

$$i\hbar \frac{\partial}{\partial t} \Psi(t) = -\Psi^*(t) \int_{t_0}^{\infty} d\tau \Psi^2(\tau) \frac{\partial}{\partial \tau} h(t, \tau). \quad (3)$$

Here t_0 is the initial time of the pulse (see Fig. 1) and $h(t, \tau)$ is the coupling function that accounts for the interactions of the gas atoms. In Ref. [7] we have described the binary collision dynamics in terms of a single separa-

ble potential $V(t)$ that mimics the low energy scattering properties of the two component coupled-channel Hamiltonian (1) and, at each magnetic field strength $B(t)$, the long range of the $\{-2, -2\}$ component of the coupled-channel bound state (see Fig. 2). The coupling function includes the entire two-body time development operator $U_{2B}(t, \tau)$ [7] and is given by

$$h(t, \tau) = (2\pi\hbar)^3 \theta(t - \tau) \langle 0 | V(t) U_{2B}(t, \tau) | 0 \rangle. \quad (4)$$

Here $\theta(t - \tau)$ is the step function that yields 1 at $t > \tau$ and vanishes elsewhere, and $|0\rangle$ is the zero momentum plane wave. In this treatment $U_{2B}(t, \tau)$ accounts, in a unified manner, for both bound and free molecular states formed during the pulse sequence.

In Ref. [7] we have determined the number of diatomic molecules in a weakly interacting gas in terms of the quantum mechanical observable [16] that counts, for each of the $N(N - 1)/2$ pairs of atoms in a gas with N atoms, the overlap between the molecular bound state wave function and the many-body state. We have shown explicitly in Ref. [7] that, despite the N^2 scaling behavior of the number of pairs of atoms, our microscopic many-body description predicts the number of diatomic molecules to be smaller than $N/2$, as soon as $n_0 a^3 \ll 1$. According to Ref. [7], for a homogeneous gas, the amplitude of the density of the molecular fraction is given by

$$\Psi_b(t) = \frac{1}{\sqrt{2}} \int d^3r \phi_b^*(r) [\Phi(\mathbf{r}, t) + \Psi^2(t)]. \quad (5)$$

Here t is the time at which the molecules are detected (and thereby destroyed), and

$$\Phi(\mathbf{r}, t) = -(2\pi\hbar)^{\frac{3}{2}} \int_{t_0}^t d\tau \Psi^2(\tau) \frac{\partial}{\partial \tau} \langle \mathbf{r} | U_{2B}(t, \tau) | 0 \rangle \quad (6)$$

is the pair function [7, 11]. The densities of the molecular fraction and the atomic condensate are then obtained by $n_b(t) = |\Psi_b(t)|^2$ and $n_c(t) = |\Psi(t)|^2$, respectively.

Figure 3 shows the evolution of the atomic condensate density and the molecular fraction in a homogeneous gas with a density of $n_0 = 3.9 \times 10^{12} \text{ cm}^{-3}$ for different evolution times of the magnetic field pulse sequence in Fig. 1. As explained above, the molecular fraction is physically meaningful only at the beginning ($t_0 = 0$) and end ($t_{\text{fin}} = 84, 85, 86, 87 \mu\text{s}$ in Fig. 3) of the pulse sequence as well as in the evolution period (beginning at $37 \mu\text{s}$ in Fig. 3). At $t_0 = 0$ the gas is prepared as a pure atomic condensate so that $n_b(t_0) = 0$. The final densities $n_c(t_{\text{fin}})$ and $n_b(t_{\text{fin}})$ exhibit the experimentally observed [4] pronounced oscillations depending on the evolution time t_{evolve} (see Fig. 1), with a frequency $|E_b(B_{\text{evolve}})|/\hbar$ and a relative phase shift depending on the relative magnitudes of all components of the gas. The amplitude of the oscillation in $n_b(t_{\text{fin}})$ is about twice the near constant molecular fraction in the evolution period

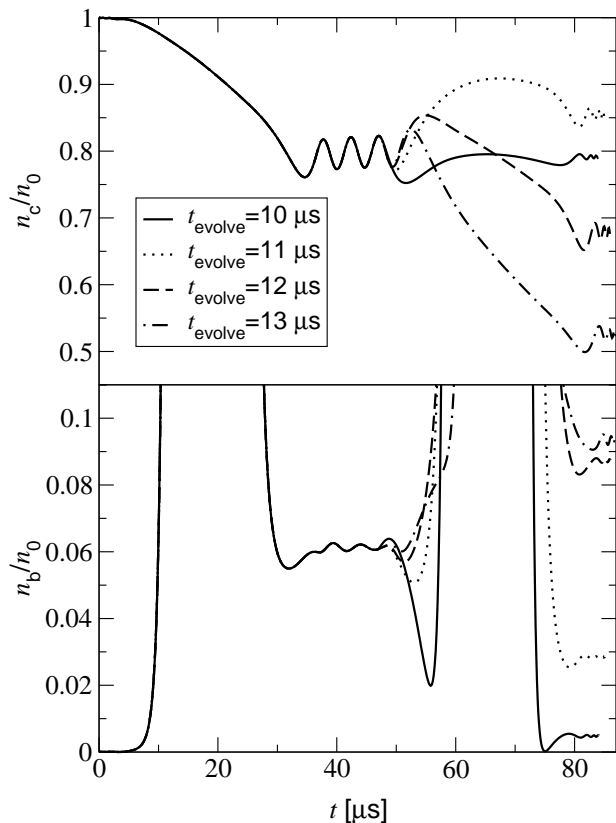


FIG. 3: Evolution of the densities of the atomic condensate n_c and the molecular fraction n_b for different evolution times of the magnetic field pulse sequence in Fig. 1 ($t_{\text{evolve}} = 10, 11, 12, 13 \mu\text{s}$). The initially pure homogeneous ^{85}Rb condensate has a density of $n_0 = 3.9 \times 10^{12} \text{ cm}^{-3}$.

of $n_b/n_0 = 6\%$. The small oscillations in n_c and n_b during the evolution period in Fig. 3 indicate the small $(n_0[a(B_{\text{evolve}})]^3)^3 = 8 \times 10^{-5}$ but finite overlap between the atomic condensate and the molecular fraction. At the lowest value of the field pulses in Fig. 1 one obtains $n_0[a(B_{\text{min}})]^3 = 0.27$ and the observable that determines the number of bound pairs in a weakly interacting gas even yields $n_b > n_0/2$ (not shown explicitly in Fig. 3). This clearly indicates the significant overlap between the molecular wave function of a pair of atoms with its surrounding gas atoms. The gas is then described by a strongly correlated non-stationary many-body state.

The entire dynamics of the different components of the gas can be understood in an intuitive way when the linear ramps of the two field pulses in Fig. 1 are idealized as sudden switches of the magnetic field strength. The first field pulse then shifts the virtually uncorrelated initial condensate into a many-body state with the crucial binary correlations. The overlap of this many-body state with the multi-channel bound state of the pairs of atoms at the field strength B_{evolve} determines the molecular fraction in the evolution period. The overlap with the

corresponding excited binary scattering states provides a first burst fraction [4, 7] of correlated pairs of comparatively hot atoms. In the evolution period the atomic condensate and the molecular component are virtually orthogonal and evolve coherently. At the end of the evolution period the difference in phase between the amplitude of the atomic condensate and the molecular fraction is $\Delta\varphi = E_b(B_{\text{evolve}})t_{\text{evolve}}/\hbar$. The second field pulse gets both components to overlap and, thereby, probes their phase difference. The second burst fraction as well as the final atomic condensate and molecular component thus exhibit an interference depending on $\Delta\varphi$. As the field pulses are chosen as mirror images in Fig. 1, at constructive interference, $n_b(t_{\text{fin}})$ can be expected to result in about twice the molecular density in the evolution period.

We have shown in this letter that highly excited diatomic bound states produced in recent experiments [4] are characterized by a large spatial extent that by far exceeds the size of all known ground state molecules [17]. The corresponding $^{85}\text{Rb}_2$ wave functions are strongly dominated by their $\{-2, -2\}$ open channel component. We have analyzed the non-adiabatic association mechanism of Ref. [4] on the basis of a microscopic quantum mechanical many-body description of the gas. Our predicted molecular fraction of 6% in the evolution period of the pulse sequence [4] exceeds the results of Ref. [5] by more than an order of magnitude. This provides a significantly better perspective for proposed experimental schemes to detect the molecules. Corrections imposed by the atom trap [7] do not affect the orders of magnitude reported here. Their systematic study in connection with possible improvements of molecular production schemes will be subject to future work.

We thank Eleanor Hodby, Neil Claussen, Simon Gardiner and Bill Phillips for inspiring discussions. This work was supported by the U.K. EPSRC (T.K.). K.B. is a Royal Society Wolfson Merit Award holder.

-
- [1] R.H. Wynar *et al.*, *Science* **287**, 1016 (2000).
 - [2] J. Stenger *et al.*, *Phys. Rev. Lett.* **82**, 2422 (1999).
 - [3] S.L. Cornish *et al.*, *Phys. Rev. Lett.* **85**, 1795 (2000).
 - [4] E.A. Donley *et al.*, *Nature (London)* **417**, 529 (2002).
 - [5] S.J.J.M.F. Kokkelmans and M.J. Holland, *Phys. Rev. Lett.* **89**, 180401 (2002).
 - [6] M. Mackie, K.-A. Suominen, and J. Javanainen, *Phys. Rev. Lett.* **89**, 180403 (2002).
 - [7] T. Köhler, T. Gasenzer, and K. Burnett, *Phys. Rev. A* **67**, 013601 (2003).
 - [8] References [5, 6] separate out physical observables associated with diatomic bound states in terms of a phenomenological quantum field that is included in the Hamiltonian. The molecular fraction reported in [5] is less than 0.5% throughout the evolution period of the pulse sequence and rises steeply at the final ramp. The

results in this letter will exceed these predictions by more than an order of magnitude.

- [9] E. Braaten, H.-W. Hammer, and M. Kusunoki, e-print arXiv cond-mat/0301489.
- [10] Private communication from Eleanor Hodby and Neil Claussen.
- [11] T. Köhler and K. Burnett, Phys. Rev. A **65**, 033601 (2002).
- [12] This is the long range asymptotic form of the free Green's function evaluated at the near resonant binding energy $E_b = -\hbar^2/ma^2$ (see, e.g., [7]).
- [13] J.L. Roberts *et al.*, Phys. Rev. A **64**, 024702 (2001).
- [14] F.H. Mies, E. Tiesinga, and P.S. Julienne, Phys. Rev. A **61**, 022721 (2000).
- [15] J. Fricke, Ann. Phys. (N.Y.) **252**, 479 (1996).
- [16] For a general description of the detection of composite particles see, e.g., J. D. Dollard, J. Math. Phys. **14**, 708 (1973).
- [17] The bond length of the largest known diatomic ground state molecule ${}^4\text{He}_2$ is of the order of $100 a_{\text{Bohr}}$ [see R.E. Grisenti *et al.*, Phys. Rev. Lett. **85**, 2284 (2000)].